

EROSION OF A LARGE-SCALE GASEOUS STRATIFIED LAYER BY A TURBULENT JET – SIMULATIONS WITH URANS AND LES APPROACHES

A. Kraus, S. Aithal, A. Obabko, E. Merzari

Argonne National Laboratory
9700 S Cass Ave., Argonne, IL 60439, USA
arkraus@anl.gov; aithal@mcs.anl.gov; obabko@mcs.anl.gov; emerzari@anl.gov

A. Tomboulides*

Department of Mechanical Engineering
Western Macedonia University
Pl. Agiou Dimitriou, Kozani 501 00, Greece
ananiast@enman.auth.gr

P. Fischer*

Department of Computer Science and Department of Mechanical Science and Engineering
University of Illinois at Urbana-Champaign
901 West Illinois Street, Urbana, IL 61801, USA
fischerp@illinois.edu

ABSTRACT

In light of the Fukushima accident, significant research effort has been focused on containment thermal-hydraulics and gaseous mixing. In one such effort, the recent OECD/NEA—PSI Computational Fluid Dynamics (CFD) Benchmark “PANDA”, an initially stratified air-helium layer is gradually eroded by a turbulent round jet ($Re = 20000$) of primarily air. Mole fraction and temperature readings were taken at various points throughout the domain to record the erosion behavior, and mean and RMS velocity profiles were averaged over a long transient time. These data were the basis for comparison with CFD results from Unsteady Reynolds-Averaged Navier-Stokes (URANS) and Large-Eddy (LES) simulations. URANS two-species simulations were run with STAR-CCM+ focusing on the Realizable $k-\epsilon$ turbulence model and low-Mach approximation under ideal gas conditions. The LES calculations were performed with the spectral-element open-source highly-scalable code Nek5000 using both a Boussinesq and low-Mach-number approximation that involved a new computational framework for handling multi-species diffusion and transport. URANS results for the mole fractions over time and averaged flow profiles showed reasonable agreement with the available experimental results for nearly all available measurements. The initial LES results demonstrated the new code capability and some early-time behavior restricted by long integration time due to a vast range of spatial and temporal scales. Nevertheless, these results can be used to improve turbulence modeling for the URANS approach that as shown here is an appropriate tool for future analyses of this type of transient flow.

KEYWORDS

turbulent jet, stratification erosion, species mixing, large eddy simulation, low-Mach number

* Joint appointments with Argonne National Laboratory

1. INTRODUCTION

Erosion of a stable gaseous layer in a containment vessel by buoyant jets is a problem of great importance in nuclear reactor safety and risk analyses. Understanding the underlying physical mechanisms and dynamics of these phenomena can play an important role in the design, analyses and risk mitigation in nuclear reactors. With this objective in mind, the third International Benchmark Exercise (IBE-3) conducted an experimental study to gather data addressing the erosion of a stratified layer by an off-axis buoyant jet in a large vessel. A dedicated experiment in the PANDA facility was conducted at the Paul Scherrer Institut (PSI) in Switzerland. In order to simplify the understanding of the physical phenomena, helium was used as the buoyant gas (instead of hydrogen) and air was used instead of steam. Since the complex physics associated with steam condensation effects were eliminated by this choice of gases, the experimental data were deemed to be suitable for blind CFD validation exercises.

The above benchmark experiment is described in detail in [1] and only briefly discussed here for the benefit of the reader. The test was conducted in a single eight meter tall vessel at the PANDA facility. The test was initiated with a helium-air layer that occupied the top two meters of the vessel and pure air in the lower part. The helium-rich layer was gradually eroded by a low-momentum air/helium jet emerging from an off-axis inlet placed 3 m below the helium-air layer as shown in Fig. 1. The experiment was conducted under ambient pressure and temperature conditions, while the temperature of the injected gases was slightly higher.

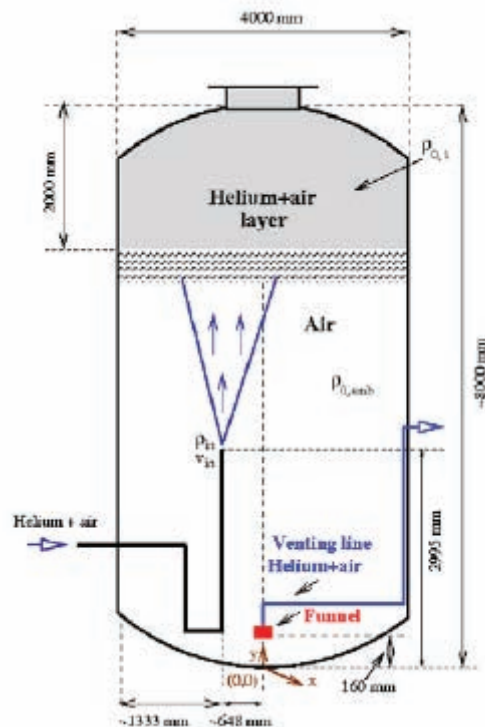


Figure 1. Schematic of the PANDA test, reproduced from [2].

Temporal variations of molar concentration and temperature, as well as time-averaged mean and RMS vertical velocity component, were measured along specified horizontal and vertical lines as explained in [1]. The experiment was conducted for nearly two hours (7200 s). Nineteen different groups participated in this OECD benchmark exercise. Nearly all simulations were conducted using commercial codes such

as CFX, FLUENT, and STAR-CD, and most of them used second-order spatial differencing [2]. Nearly half of the participants used the standard Unsteady Reynolds-Averaged Navier-Stokes (URANS) two-equation turbulence modeling approach (variants of the well-established k - ϵ and k - ω models), with mesh sizes ranging from 400,000 to 2.2 million cells. The other half used turbulence modeling approaches such as LES, Scale-Adaptive Simulation (SAS), Reynolds-Stress Model (RSM) or standard modeling on a coarse mesh (the largest mesh was 4.3 million cells). The general conclusion of the above benchmark was that even for the simple flow, there was an unexpectedly large spread of the main variables between various users. The choice of the modeling approaches and grid resolution were identified as important plausible reasons for this discrepancy.

This work seeks to address some of the plausible causes of discrepancy between experimental data and numerical simulations. The primary focus of this work was to conduct a systematic study of the PANDA experiment using URANS in the commercial code STAR-CCM+ [3] and a well-resolved ($>40M$ degrees of freedom) LES simulation using an open source, high-order spectral element code, Nek5000 [4-5]. Such a study would enable the evaluation of trade-off between accuracy and computational time between the URANS and LES approaches using high-order methods.

2. URANS SIMULATIONS

2.1. Methods

The initial goal for the URANS simulations was to establish a basic solution approach. From this case, parametric studies could be performed to find optimal conditions for replicating the experimental behavior. A geometry file was constructed to reflect the PANDA vessel dimensions. In order to simplify meshing, a number of small protrusions were neglected and the “funnel” outlet [1] was instead replaced by a tapered outlet at the bottom of the vessel. The tapering accelerates the flow and helps to prevent recirculating flow at the outlet, which can cause numerical issues. Given that measurements of the velocities, turbulence parameters, and molar fractions slightly above the inlet pipe were provided in [1], flow in the inlet pipe was not explicitly calculated. The pipe length was shortened and served primarily to topologically separate the inlet surface from the rest of the tank.

Meshing was performed within STAR-CCM+ using a trimmed meshing model, which produces primarily hexahedral cells which are trimmed on the domain boundaries by a prismatic layer [3]. A cone of refinement was included in the jet region, with a width roughly corresponding to the theoretical spreading rate of the jet. Two primary meshes were used, the “base” mesh consisting of ~ 1.3 million cells and the “coarse” mesh consisting of $\sim 290,000$ cells (Fig. 2). The only difference between these two meshes was the level of refinement in the jet area. Intermediate meshes showed that refinement outside of the jet area did not have much impact on the mole fraction predictions.

STAR-CCM+ was used to solve the equations for flow and heat/species transfer. It employs a finite-volume approach. A second-order upwind formulation was used to discretize the convective terms. The implicit Coupled Flow and Coupled Energy models were used and yielded good, smooth convergence behavior [3]. An ideal gas equation of state was used. A Low-Mach number formulation was employed, for which the equation of state is independent of the pressure.

Simulation time was taken to start with the onset of flow exiting the inlet pipe. Time-stepping was performed using an implicit second-order Euler method. For most simulations, the initial time step was 0.01s, increasing gradually to 0.05s at 4s of simulation time. This corresponded to a Courant number of ~ 50 in the jet region. For the base case, a comparison case was run with a uniform time step of 0.005s. The results were nearly identical to those of the larger time-step case, providing evidence that the approach was appropriate.

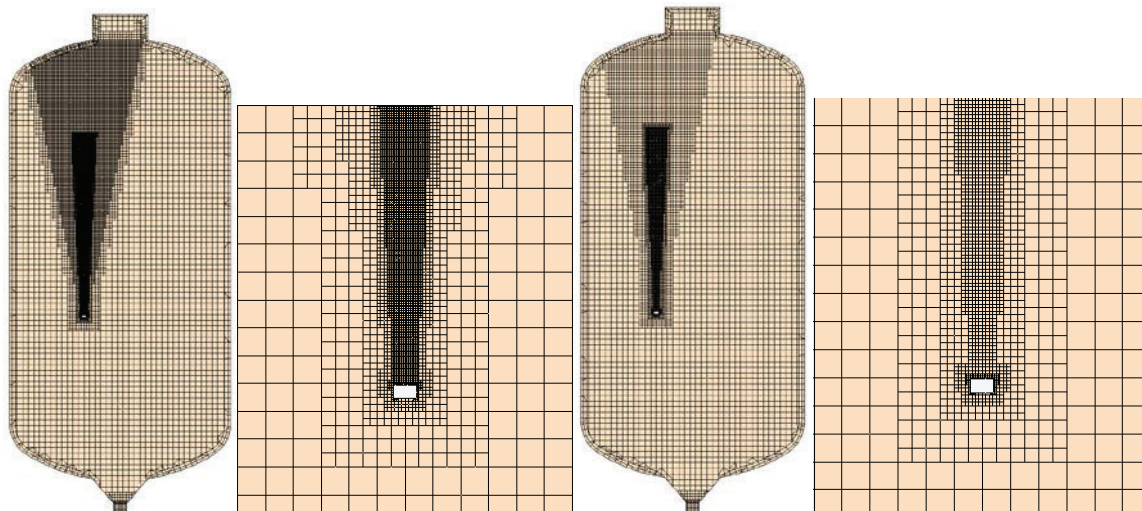


Figure 2. Base mesh (left) and coarse mesh (right), with zoomed in views of the inlet pipe region.

A constant mass flow inlet condition was used in conjunction with a constant pressure outlet condition. The temperature and mole fraction data for the initially stratified conditions in the vessel were directly applied to the mesh from the data in [1]. Polynomial correlation trendlines were drawn for the data from mean and RMS velocity measurements taken slightly above the inlet [1]. These correlations were applied as boundary conditions at the inlet based on the radial coordinate from the pipe center. The inlet flow is gradually heated, which was taken into account, but the vessel walls were treated as adiabatic. This means that the fluid temperatures in the vessel will gradually increase over the entirety of the simulation, which is not in agreement with the experimental data. However, the temperature range is only $\sim 9\text{K}$, and so the influence of this temperature difference on flow behavior is presumed to be small.

Two-species simulations were performed to simulate the transport and diffusion of the air and helium. The inlet air contained some water vapor, but it was a small enough fraction that it was not included in the simulations. Fluid properties were used based on mass- and mole-weighted values of those of the individual gases. The binary diffusion coefficient was $6.98 * 10^{-5} \text{ m}^2/\text{s}$, while the turbulent Schmidt number was taken to be a constant value of 0.9, the default value in STAR-CCM+. Ranges of 0.7-0.9 were recommended by [6] for a free jet flow.

Initial turbulence modeling was performed with the Realizable Two-Layer $k-\epsilon$ model [7], which is the default RANS model provided in STAR-CCM+ and uses adaptive wall modeling. One reason for choosing this model over the SST model that many benchmark participants used is that in the STAR-CCM+ implementation, there is no explicit incorporation of buoyancy effects in SST. Default coefficients were used for the initial simulations. The default approach tends to set the coefficient of the buoyancy production of dissipation term to zero outside of natural convection boundary layers [3]. As boundary layers are not of prime importance for the free jet, a second approach was to use a “thermal stratification” formulation, where the coefficient is set to unity in areas with positive buoyancy production and set to zero in areas with negative buoyancy production. Given the importance of stratification in this experiment, the second approach should be expected to be more accurate, but should be tested.

Another, somewhat more advanced turbulence modeling approach is to use RSM. Only one participant in [2] used RSM, so the authors feel that a more systematic investigation would better highlight the merits of using RSM for this problem. The specific variant of RSM used here is the “SSG” quadratic pressure-strain model [8]. In this model, the Reynolds stresses are all transported individually, which can account for effects like anisotropy and streamline curvature. This is in contrast to the Realizable Two-Layer $k-\epsilon$

model, which assumes isotropic turbulence. This attribute may be beneficial for simulating this experiment, in which there is elevated turbulence in the axial direction. The Daly-Harlow General Gradient Diffusion Hypothesis (GGDH) was employed [9]. It incorporates anisotropic Reynolds-stress diffusion, as opposed to the frequently-used isotropic assumption, and has been shown to be more accurate for computing scalar fluxes [10]. However, there are still uncertainties in the model, and RSM features an increased computational cost, so its usefulness for this type of flow should be assessed.

It should be noted that the top four best-ranking simulations in [2] used either SST or SAS-SST, included heat transfer at the vessel wall, and included the inlet pipe surface (and possibly other geometric details). Thus the approach used here attempts to show that the omissions and simplifications described above are valid and that SST and $k-\epsilon$, both being two-equation models, should theoretically be able to produce reasonably similar results for this relatively simple flow. Moreover, STAR-CCM+ was not tested by any participants (although STAR-CD was used by one group), so this is a useful benchmark for the code itself.

The authors would like to emphasize the importance of obtaining good simulation results for velocity. Benchmark results showed that reasonable estimation of helium drop did not always coincide with good velocity results [2]. It is clear that diffusion plays a significant role in the mole fraction behavior, and a fortuitous combination of mesh size, diffusion coefficient, time step size, etc. could work to achieve reasonably accurate erosion while getting other aspects of the general flow behavior wrong. For this reason, an emphasis is placed on getting both the velocity and erosion reasonably correct in this work.

2.2. Initial Results and Mesh Comparison

Results from the initial simulations for the base mesh display reasonable agreement with the measurements presented in [2]. It must be noted that the full data from the benchmark had not been released at the time of this work, so the points in [2] are the only data available to gauge accuracy of the simulation. Mole fraction data presented here correspond to “quench” positions above the inlet at points B_18, C_18, CDA_118, CDA_218, DE_18, and F_18 (Fig. 3). The left-most measuring point is closest to the inlet pipe and the right-most measuring point is furthest. The mean and RMS velocity data correspond to “VVy_1”, “TKE_1”, “HVy_3”, and “HVyRMS_3” (clockwise from top left in Fig. 4). The times and locations of all of these can be found in [1]. Generally speaking, these measurements are all taken directly above the inlet pipe. As a reference point, the pipe outlet is centered at -0.648m, 2.995m, 0.0m (see Fig. 1). In all mole fraction graphs, points of a similar color correspond to the same measuring point.

The main behavior of the helium erosion process (Fig. 3) is captured in the base model, with the erosion time generally occurring faster in the simulation than in experiment. Errors are higher for the highest elevations. Horizontal velocity is captured very well, and RMS is underestimated in the center but still well approximated (Fig. 4). Vertical velocity is good near the inlet but becomes less accurate with increasing elevation. The vertical turbulent kinetic energy (TKE) agrees well in the measurement region.

This simulation was repeated using the coarse mesh, and the erosion process was found to be very similar. For short to medium times, the helium drop behavior was almost identical between the two simulations (Fig. 3), while the erosion times for the uppermost monitoring points were found to be slightly longer for the coarse mesh. Given this excellent agreement and the savings in computational time, the coarse mesh was used for all ensuing calculations.

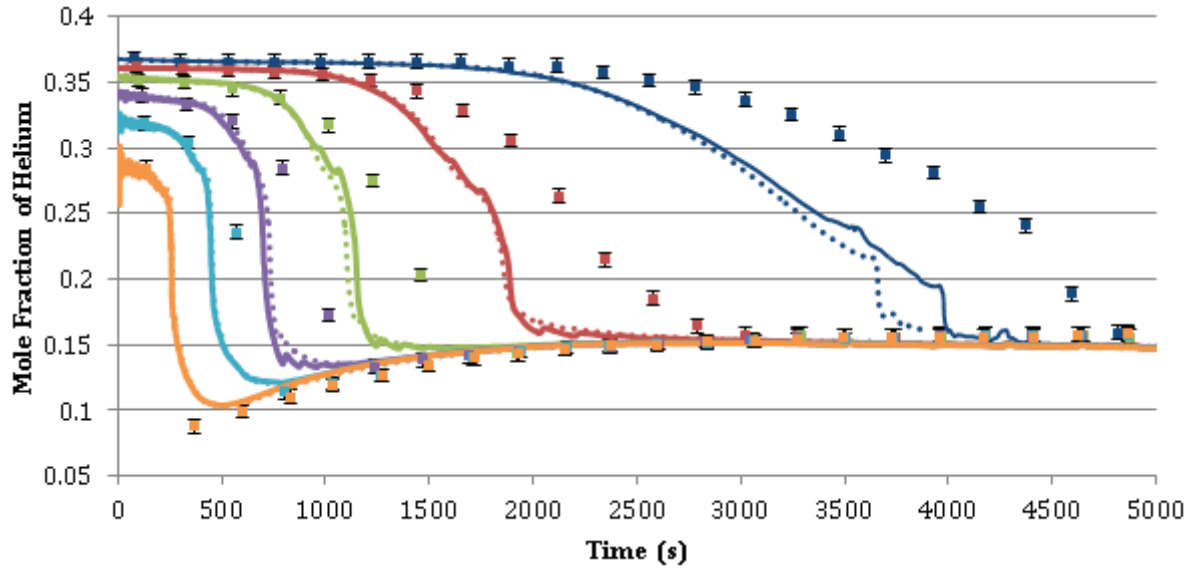


Figure 3. Helium drop comparison between experiment (points), base mesh (dotted), and coarse mesh (solid). Lines of the same color correspond to the same measuring point.

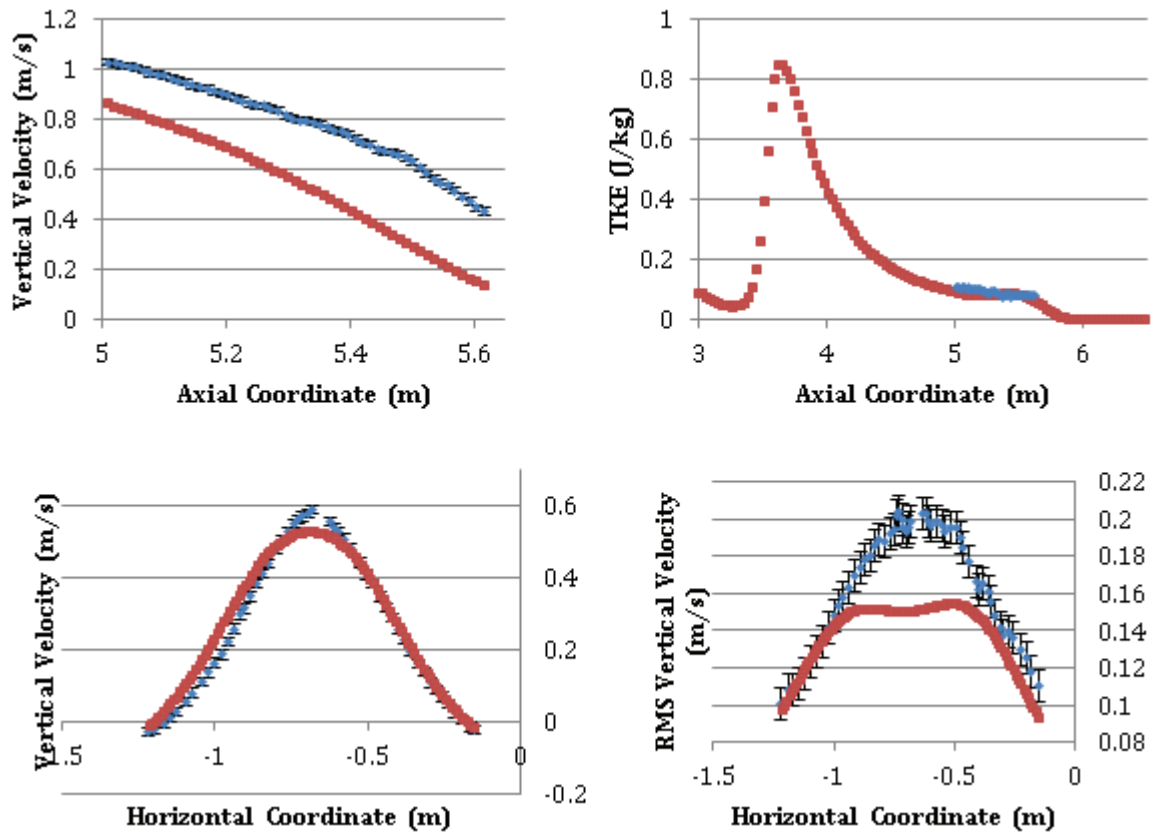


Figure 4. Clockwise from top left, comparisons of vertical velocity axial profile, TKE, and RMS and mean vertical velocity horizontal profiles compared with experimental values. Red is simulation, blue is experiment.

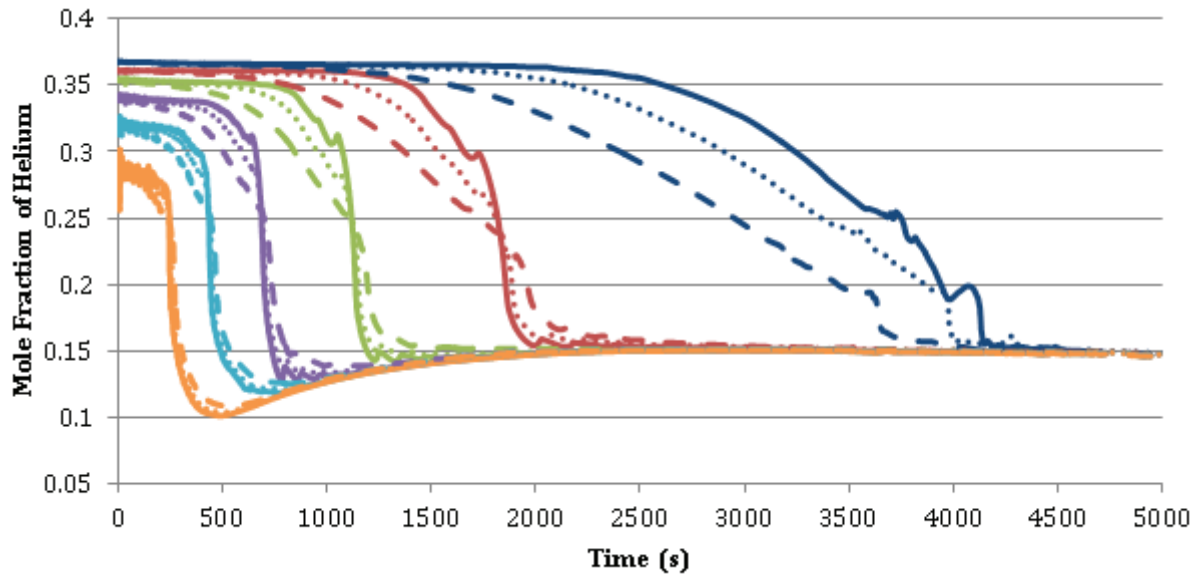


Figure 5. Comparison of molecular diffusion coefficients, with dotted as standard, solid as 2x lower, and dashed as 2x higher.

2.3. Diffusion and Turbulent Schmidt Parametric Studies

Studies were undertaken to determine the influence of the diffusion coefficients and turbulent Schmidt numbers, since these varied significantly between participants. Simulations were performed with the diffusion coefficient magnitude roughly two times higher (3.5×10^{-5}) and two times lower (14×10^{-5}) than in the base simulation. Turbulent Schmidt numbers of 0.7 and 1.5 were investigated. The molecular diffusion coefficient has a relatively minor effect on the overall concentration behavior (Fig. 5). The results suggest that higher diffusion yields a faster gradual decay of the helium, but that it is not a large factor in the catastrophic drop to the “quench” level, which is presumably caused more by jet interaction. This is particularly evident at the lower elevations.

The turbulent Schmidt number effect was evident for each measurement point at the onset of noticeable erosion. The erosion with the turbulent Schmidt value of 1.5 took longer than in the base cases, but the shape of the graph is still similar. For the 0.7 value, erosion took place somewhat faster than the base case (Fig. 6), but not strongly so. Thus the turbulent Schmidt number is unlikely to be a major source of the discrepancies in [2]. As expected, a higher turbulent Schmidt leads to more momentum diffusion than concentration diffusion, and the erosion process occurs more slowly. Many benchmark participants used a value of 0.7, which could be part of the reason why the erosion times were frequently underestimated in the benchmark.

2.4. Thermal Stratification Buoyancy Production

As anticipated, implementing the thermal stratification buoyancy coefficient increased the accuracy of the simulation. Fig. 7 demonstrates that the erosion time has indeed been lengthened, which results in increased accuracy, particularly at the higher elevations. Velocity profiles throughout are essentially the same as for the default model. Given the quality of these results for both erosion and velocity, the settings used in this simulation were deemed to be appropriate to solve this problem reasonably accurately. Thus any significant increase in computational time past this level would have to be warranted by a profound increase in accuracy.

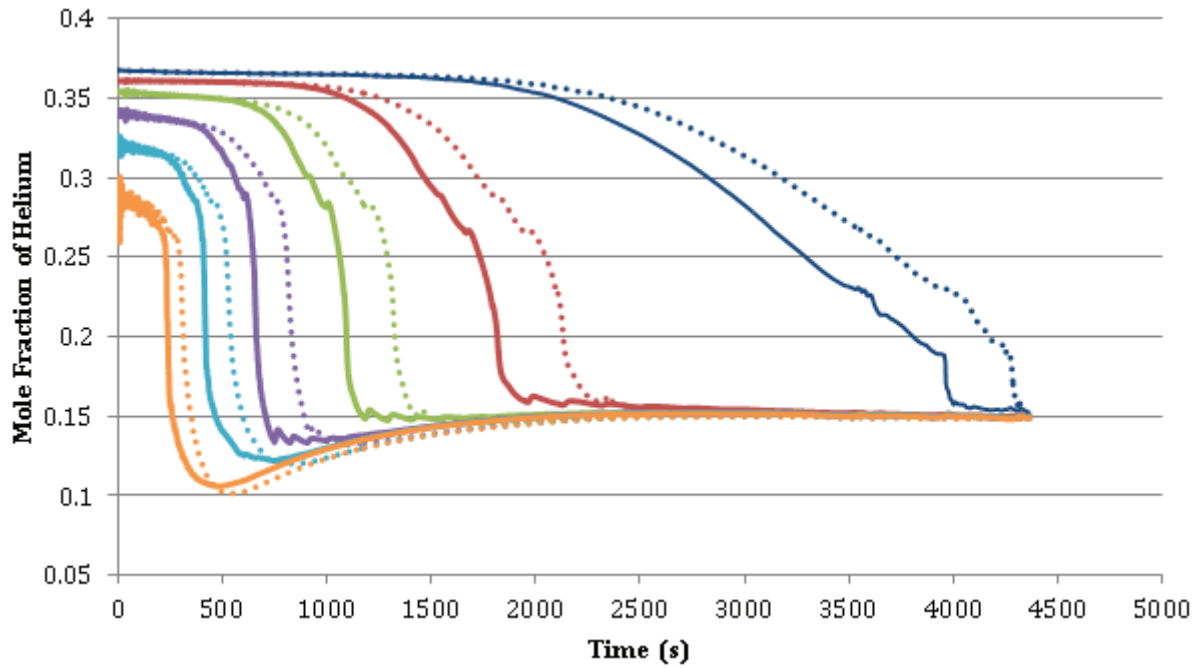


Figure 6. Turbulent Schmidt number comparison, solid lines are 0.7 and dotted lines are 1.5.

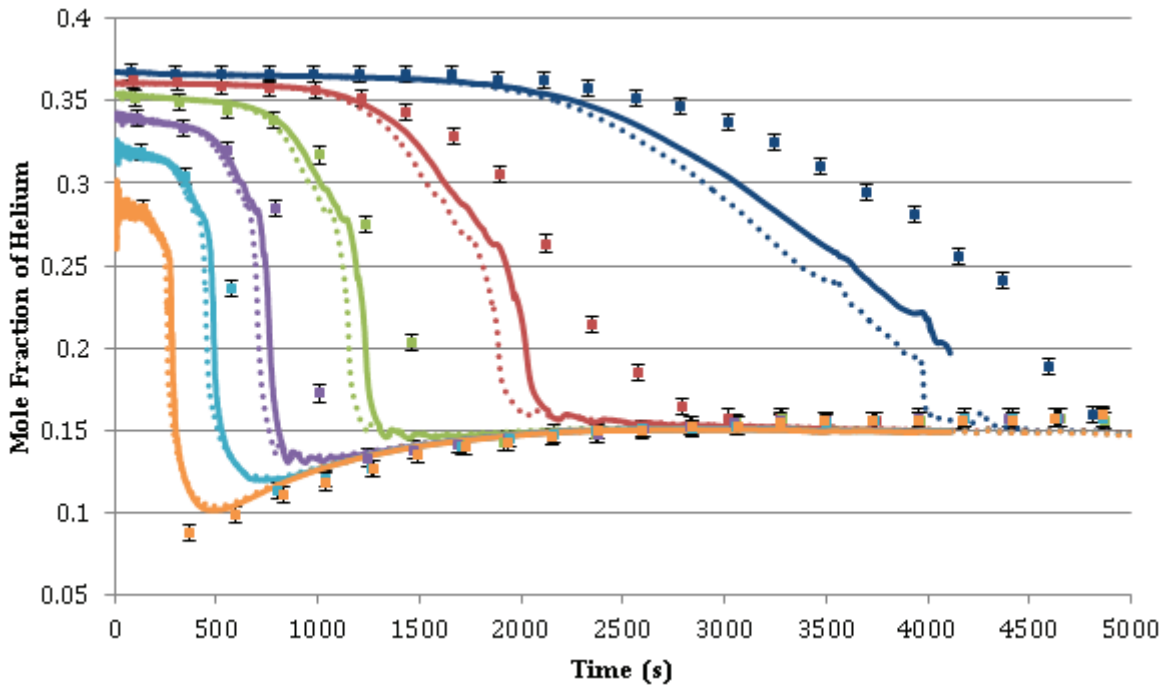


Figure 7. Comparison of experiment (points), coarse mesh default (dotted), and coarse mesh with thermal stratification approximation (solid).

2.5. RSM Simulations

Results from the RSM simulations were reasonably accurate and offered some improvement over the Realizable Two-Layer $k-\epsilon$ model, particularly for erosion behavior. The models are compared in Figs. 8-9. Firstly, the erosion behavior is rather good, and the temporal behavior is very close to experiment, especially at lower elevations. The RSM predicts, however, longer erosion times on average than those found in experiment, so it is not “conservative” for estimating erosion. This conservative behavior can be desirable in the context of safety applications. Erosion time for the top point in particular is well overestimated. Secondly, the mean velocity data are worse but RMS velocity data are better for RSM. The horizontal and vertical velocities are both lower, while the TKE is higher. It was found that the base mesh was required to obtain resolved values for the RMS, which are notably an improvement over $k-\epsilon$.

The need for the base mesh, however, leads to a significantly increased computational cost for RSM. Thus it is debatable whether the higher-fidelity RSM provides an all-around improvement in results to warrant its increased computational cost. Further investigation should be performed for improving its behavior at the higher elevations. Additional RSM variants could also be investigated.

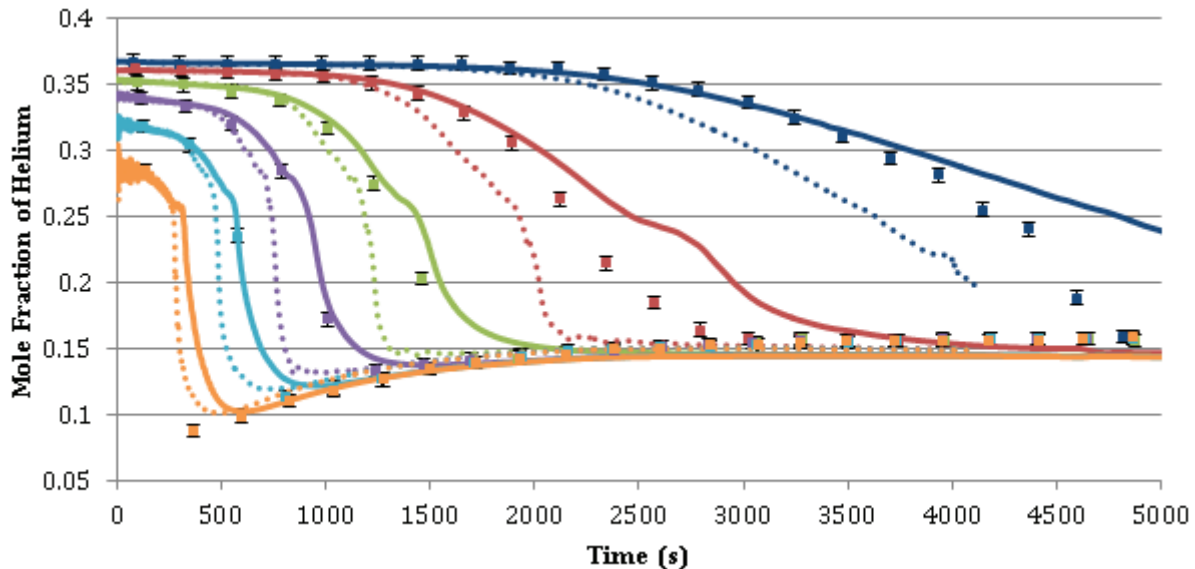


Figure 8. Helium concentration behavior for experiment (solid), $k-\epsilon$ with stratification (dashed), and RSM (dotted).

2.6. Computational Cost Comparison

For the URANS simulations, the computational cost was estimated from the number of iterations, the average solver CPU time per iteration, and the time step size. While the cost magnitude will vary from machine to machine, the ratio between two of the simulations should be a good indication of relative performance. The cost in core-days for each of the simulations was roughly 700 for the base mesh $k-\epsilon$, 190 for the coarse-mesh $k-\epsilon$, and 1266 for the base-mesh RSM. This means that for $k-\epsilon$ the base mesh takes $\sim 3.7x$ longer than the coarse mesh with similar results. The RSM takes $\sim 1.8x$ longer than the base-mesh $k-\epsilon$ and $\sim 6.7x$ longer than the coarse mesh $k-\epsilon$. These emphasize the attractiveness of the coarse-mesh $k-\epsilon$ for simulating this problem. The time for the $k-\epsilon$ model is also lower than many of the top-ranking benchmark submissions, while also yielding as good or better results.

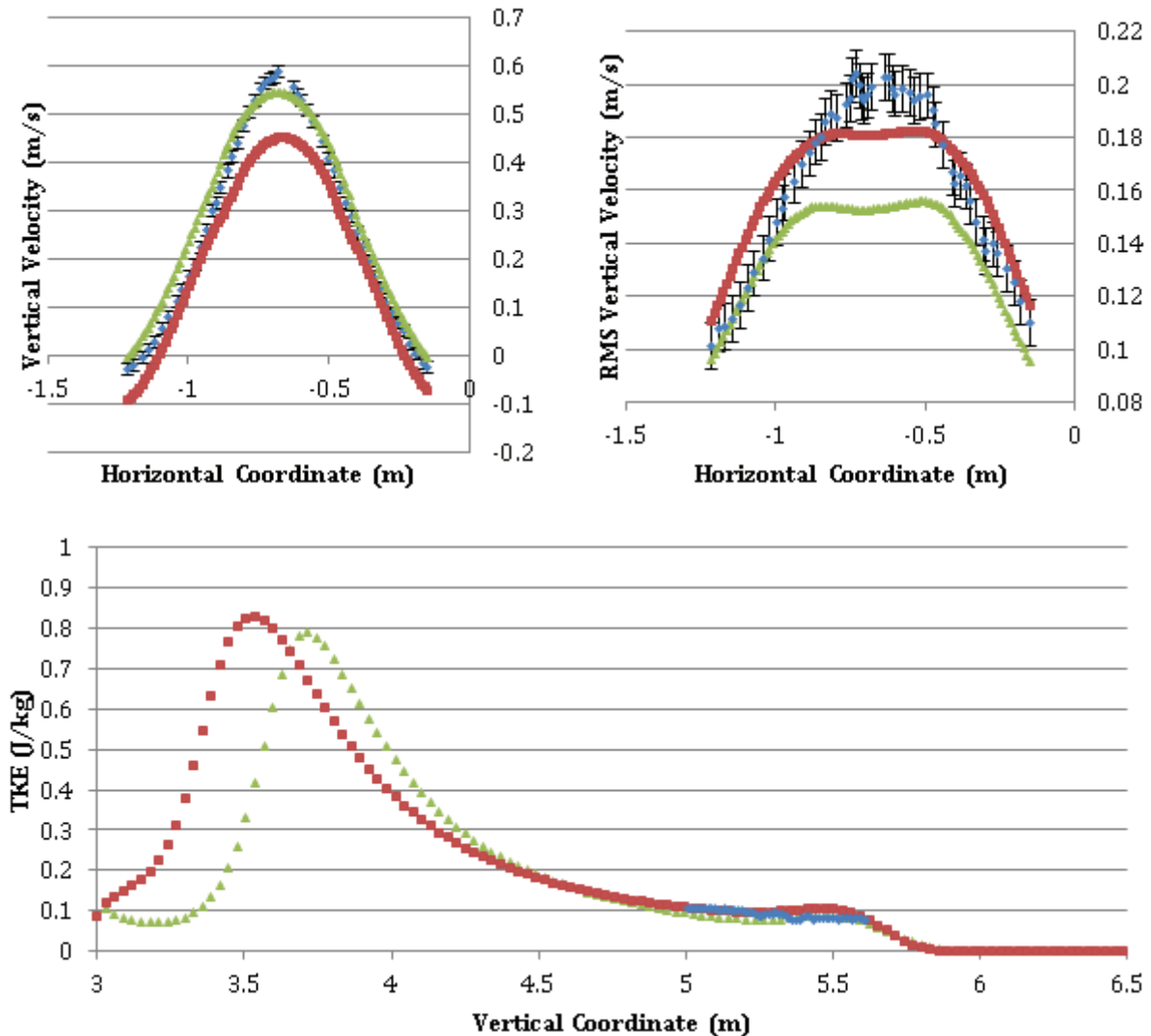


Figure 9. Clockwise, comparison of mean and RMS axial velocity, and TKE. Blue is experiment, red is RSM, green is k- ϵ stratified model.

3. LES SIMULATIONS

3.1. Methods

As discussed earlier, the flow-field of a high-speed off-axis jet emanating from a narrow inlet and discharging into a large quiescent tank is inherently unsteady. Furthermore, as the jet diffuses and mixes with the quiescent gas, the extent and location of the mixing interface between the jet and the surrounding gas is continuously changing. These flow characteristics make CFD simulations particularly challenging. URANS simulations, while providing important time-averaged flow features, do not resolve the anisotropic vortical structures associated with the mixing and diffusion process. LES, by virtue of the fact that it enables spectral filtering, is able to capture these vortices to a large extent. LES simulations are thus able to provide a more realistic picture of the transient nature of the flow, albeit at a higher computational cost. Fig. 10 shows the difference between the instantaneous flow-field as represented in

URANS vs. LES. Definition of flow structures within the jet is far greater for LES, while the URANS representation is smoother.

The higher cost for LES is due not only to the finer grid resolution required but also to the smaller time steps required. LES provides mean values only by averaging the unsteady flow field computed with small time-step over a long sampling time. Thus, to obtain "accurate" LES simulations, one needs to pay special attention to both the mesh resolution and size of the time-step. LES resolves scales from the characteristic size of the domain down to the filter size. The filter (and grid size) must be chosen in order to resolve a substantial portion of the high wave number turbulent fluctuations. The use of high-order numerical schemes (such as spectral element methods) alleviates the stringent mesh requirements as compared to low-order numerical schemes (such as finite-volume methods). This important issue of adequate spatial and temporal resolution is overlooked in many cases, leading to inaccurate and erroneous results. Three LES simulations for the PANDA experiment were deemed to be far below expectation with the results being closer to the worst predictions than the best as noted in [2]. This conclusion is not surprising given the very low resolution of these simulations. It is seen that these simulations, conducted using finite-volume schemes, had cells between 790,000 and 4.3M. The computation time of these simulations was an order of magnitude higher than the RANS simulations and not nearly as accurate [2].

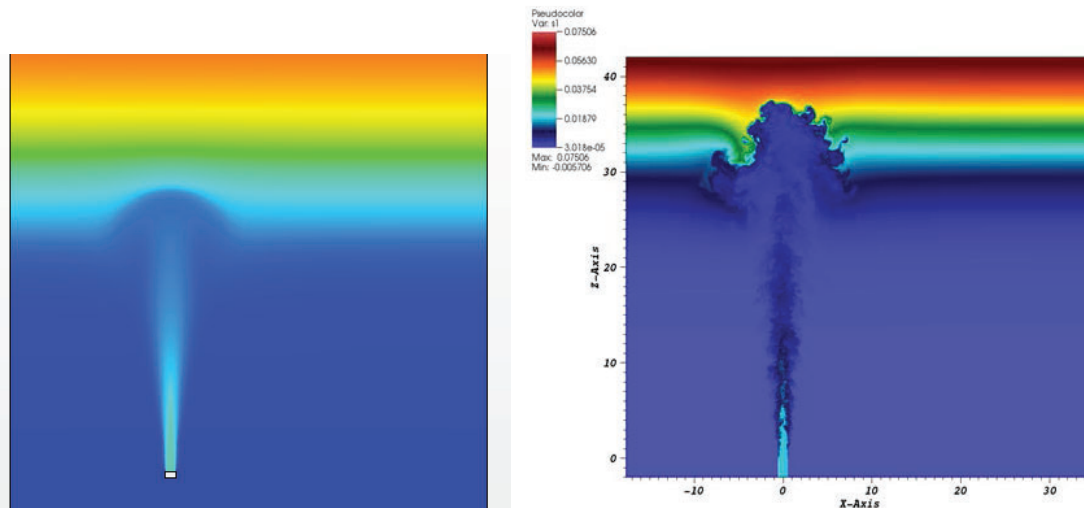


Figure 10. Comparison of URANS (left) and LES (right) instantaneous flow-field values of helium fraction (not same scale).

A more systematic approach to obtain LES solutions to the PANDA experiment is being pursued. A high-order, highly-scalable CFD solver named Nek5000 [4-5] was used to conduct high resolution simulations of the PANDA experiment on the IBM Blue Gene (BG/Q) supercomputer. A whole-vessel domain similar to that used in the URANS modeling was employed in the LES calculations. The grid topology was chosen so as to have high resolution near the inlet of the jet. Over 150,000 spectral elements were used and simulations were conducted using 7th-order polynomials. This resulted in simulations with over 40M degrees of freedom, which is roughly an order of magnitude higher than the most highly resolved LES simulation submitted to the PANDA benchmark exercise. The high degree of scalability of Nek5000 enabled the problem to be strongly scaled up to 16000 cores on BG/Q.

A new multi-species framework was implemented into Nek5000 to allow it to be able to simulate this problem. The following provide formulations for the species conservation and diffusion velocity, respectively:

$$\frac{\partial \rho Y_k}{\partial t} + \frac{\partial}{\partial t} (\rho Y_k V_k) = 0 \quad (1)$$

$$\mathbf{V}_k = \frac{1}{X_k \bar{W}} \sum_{j \neq k}^K W_j D_{k,j} \mathbf{d}_j - \frac{D_k^T}{\rho Y_k} \left(\frac{1}{T} \right) \nabla T \quad (2)$$

where

$$\mathbf{d}_k = \nabla X_k + (X_k - Y_k) \frac{1}{p} \nabla p \quad (3)$$

and ρ is density, $Y_k (X_k)$ is the mass (mole) fraction of species k , V_k is the diffusion velocity of species k , W_j is the species molar mass, p is pressure, T is temperature, and $D_{k,j}$ are the ordinary multicomponent diffusion equations and D_k^T are the thermal diffusion coefficients. These were implemented and tested in Nek5000 for the multi-species approach used in the PANDA simulations.

3.2. Preliminary Results and Ongoing Work

Two approaches, namely the Boussinesq approximation (BA) with passive scalar transport and low-Mach number two-species formulation, were used to compare the impact of solution methodology on the overall accuracy and computational time. In order to ensure temporal accuracy, the Courant number was fixed at 0.5 yielding a typical time-step size of about 1-2 microseconds. The computational time per timestep was approximately 5 seconds. Fig. 11 shows the differences at a given time for BA as well as low-Mach for two different Schmidt numbers at similar times. These show that there are significant differences for these approaches in the way that the jet interacts with the stratified layer.

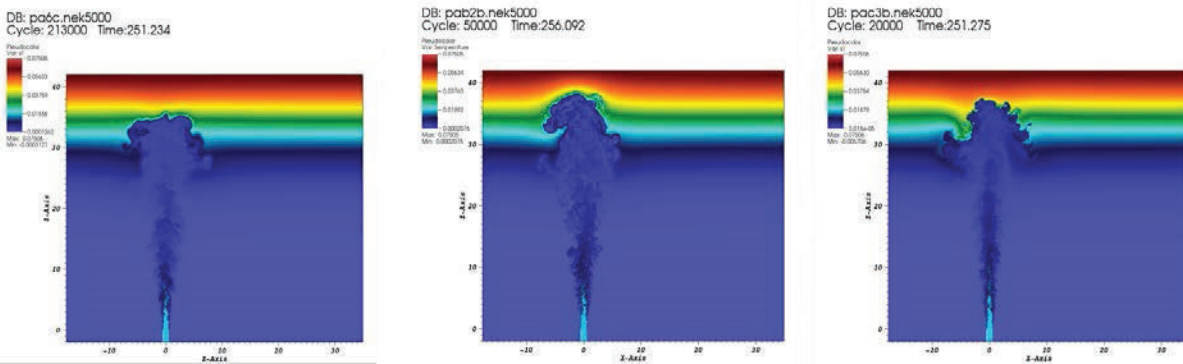


Figure 11. Comparison of Low-Mach with 1/10 Schmidt number (left), BA (middle), and Low-Mach with correct Schmidt number (right).

The primary motivation of this exercise was to obtain realistic estimates of the overall computational time, scalability and practicality of using the LES approach for the PANDA benchmark problem. Given that the experiment was conducted for 7200 seconds, it is clear that accurate LES simulations would

require an inordinately large computational time based on the required walltime per time-step. BA simulations for the first 2 minutes were conducted using about 11 million core-hours (~458,000 core-days) on BG/Q. This is clearly an enormous increase over the URANS simulations, and makes simulation of the whole transient with this approach infeasible.

However, early-time results can be used to better inform the modeling of turbulence and other physical parameters in URANS simulations. As shown above, URANS approaches can be used to simulate the PANDA experiment with reasonable accuracy, but there are a number of parameters (turbulent Schmidt number, grid resolution, etc.) that can combine to create reasonable erosion behavior, and it is still uncertain which individual values are best. Efforts are currently underway to extend LES simulations up to 215s (the end of the first velocity measurement interval) for comparison. Data from these simulations can be used to more confidently establish the strengths and weaknesses of the various URANS turbulence models, and allow for a more thorough assessment of which methods and values are most appropriate for simulating these types of transients.

4. CONCLUSIONS

The PANDA stratified layer erosion benchmark has been simulated using a number of approaches, both with URANS and LES. Reasonable agreement with experiment was obtained for coarse-mesh two-equation URANS simulations, for which computational cost was minimal. A RSM approach showed improvement in some areas but was worse in some other regards, and so the approach was not proven to warrant its increased computational cost. It was shown that good results can be obtained without modeling the inlet pipe and without heat transfer at the vessel walls. Given the relatively fast simulation time, other turbulence models could be investigated in the future to more comprehensively assess the best approach for STAR-CCM+.

LES simulations were also performed using Nek5000. Modifications to the source code allowed for multi-species simulations. Preliminary results were obtained demonstrating the new methods. It was concluded that to perform an “accurate” LES simulation of the entire PANDA transient would likely be infeasible, but that shorter-time data could be used to improve turbulence modeling for URANS simulations. Work is currently being done to perform these simulations, and improve the URANS approach for similar types of flows.

Another potential approach for this type of problem is a hybrid URANS-LES method, such as Detached Eddy Simulation. This problem should be appropriate in that it has only an isolated area featuring very turbulent flow and strong fluctuations, which is that in the immediate jet vicinity. This area would be simulated with a detailed LES-type approach, while the rest of the tank likely does not need such refined modeling and could be simulated with a URANS-type approach. This would strike a balance between the accuracy of the LES simulations and the computational cost of the URANS simulations. Further work could be performed to investigate the benefits of this type of approach.

ACKNOWLEDGMENTS

The authors would like to thank the OECD/NEA and PSI for their efforts in constructing this benchmark. This research used resources of the Argonne Leadership Computing Facility, which is a DOE Office of Science User Facility. The submitted manuscript has been created by UChicago Argonne, LLC, Operator of Argonne National Laboratory (“Argonne”). Argonne, a U.S. Department of Energy Office of Science laboratory, is operated under Contract No. DE-AC02-06CH11357. The U.S. Government retains for itself, and others acting on its behalf, a paid-up nonexclusive, irrevocable worldwide license in said article to reproduce, prepare derivative works, distribute copies to the public, and perform publicly and display publicly, by or on behalf of the Government.

REFERENCES

1. OECD/NEA--PSI CFD Benchmark Specifications, © OECD/NEA, 2013.
2. M. Andreani, A. Badillo, and R. Kapulla, "Synthesis of the OECD/NEA-PSI CFD Benchmark Exercise", *CFD4NRS5*, Zurich, Switzerland, Sep. 9–11, 2014, online.
3. CD-Adapco, "STAR-CCM+ 9.04 Manual," Melville, NY, 2014.
4. E. Merzari, W.D. Pointer, and P. Fischer, "Numerical Simulation and Proper Orthogonal Decomposition of the Flow in a Counter-Flow T-Junction," *J. Fluids Eng.*, **135** (9), p. 091304 (2013).
5. P. Fischer, J. Lottes, W.D. Pointer, and A. Siegel, "Petascale Algorithms for Reactor Hydrodynamics," *J. Phys. Conf. Ser.*, **125**, p. 012076 (2008).
6. Y. Tominaga and T. Stathopoulos, "Turbulent Schmidt Numbers for CFD Analysis with Various Types of Flowfield," *Atmos. Environ.*, **41**, pp. 8091-8099 (2007).
7. T.-H. Shih, W.W. Liou, A. Shabbir, Z. Yang, and J. Zhu, "A New k- ϵ Eddy Viscosity Model for High Reynolds Number Turbulent Flows – Model Development and Validation," NASA TM 106721 (1994).
8. C.G. Speziale, S. Sarkar, and T.B. Gatski, "Modelling the Pressure-Strain Correlation of Turbulence: An Invariant Dynamical Systems Approach," *J. Fluid Mech.*, **227**, pp. 245-272 (1991).
9. B.J. Daly and F.H. Harlow, "Transport Equations of Turbulence," *Phys. Fluids*, **13**, pp. 2634-2649 (1970).
10. R. Rossi and G. Iaccarino, "Numerical Simulation of Scalar Dispersion Downstream of a Square Obstacle using Gradient-Transport Type Models," *Atmos. Environ.*, **43** (16), pp. 2518-2531 (2009).